XRD and EBSD Measurements of Directional Solidification Fe-C Eutectic Alloy

M. Trepczyńska-Łent
Department of Materials Science and Engineering, Mechanical Engineering Faculty,
UTP University of Science and Technology, Al. prof. S. Kaliskiego 7, 85-796 Bydgoszcz, Poland
*Corresponding author. E-mail address: malgorzata.trepczynska-lent@utp.edu.pl

Abstract

In a vacuum Bridgman-type furnace, under an argon atmosphere, directionally solidified sample of Fe - C alloy was produced. The pulling rate was v = 83 μm/s (300 mm/h) and constant temperature gradient G = 33,5 K/mm. The microstructure of the sample was examined on the longitudinal section using an Optical Microscope and Scanning Electron Microscope. The X-ray diffraction and electron backscatter diffraction technique (EBSD) have been used for the crystallographic analysis of carbide particles in carbide eutectic. The X-ray diffraction was made parallel and perpendicular to the axis of the goniometer. The EBSD shows the existence of iron carbide Fe_3C with orthorhombic and hexagonal structure. Rapid solidification may cause a deformation of the lattice plane which is indicated by different values of the lattice parameters. Such deformation could also be the result of directional solidification. Not all of the peaks in X–ray diffractograms were identified. They may come from other iron carbides. These unrecognized peaks may also be a result of the residual impurity of alloy.

Keywords: X-ray diffraction, EBSD technique, Carbide eutectic, Directional solidification

1. Introduction

Several Fe-C compounds have been reported: FeC, Fe_2C, Fe_3C, Fe_3C_2, Fe_4C, Fe_5C_2, Fe_6C, Fe_7C_3, Fe_8C, $Fe_{20}C_9$, $Fe_{23}C$, and $Fe_{23}C_6$. Many of them are transitional phases or stabilized by impurity elements.

As the concentration of carbon exceeds its solubility in ferrite, accumulation of the extra carbon starts forming phases which can contain a higher amount of carbon. One of these phases is cementite, also known as iron carbide, which is a chemical compound of iron and carbon, with the formula Fe_3C, containing 6,67 wt.% carbon. Since it is a chemical compound, unlike in solid solutions, its carbon content is always fixed. It means that, in the phase diagram, the pure cementite phase exists only in a very narrow region, more accurately a vertical line, at the carbon concentration of 25,0 at.% (6,67 wt.%). Cementite has an orthorhombic crystal structure with 12 iron and 4 carbon atoms in the unit cell (Fig. 1), where experimental and theoretical studies show that the interstitial carbons prefer to occupy prismatic sites rather than octahedral sites (Fig. 1b). Mechanically, cementite is a very hard and brittle material [1].

Figure 2 shows the crystal structure of the hexagonal carbide Fe_3C (called "ε-cementite", or ε-Fe_3C). ε-Fe_3C is a metastable form of cementite Fe_3C with 16 atoms in a rhombic elementary cell [2]. In this structure, iron atoms form the HCP lattice, while carbon atoms occupy some of octopores (for short: pores) which form the simple hexagonal lattice consisting of three non-

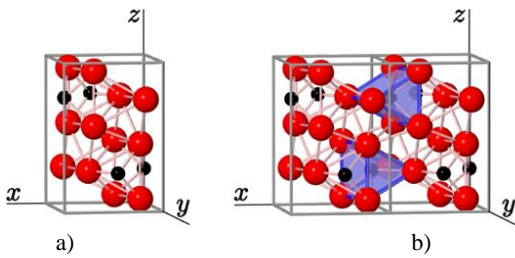equivalent sublattices, *a, b* and *d,* coloured in Figure 2 by green, blue, and yellow, respectively [2]

Fig. 1. a) Unit cell of cementite with 12 iron and 4 carbon atoms. b) Repetition of the unit cell along the x-axis shows prismatic sites occupied by carbon. Two prisms are highlighted [1]
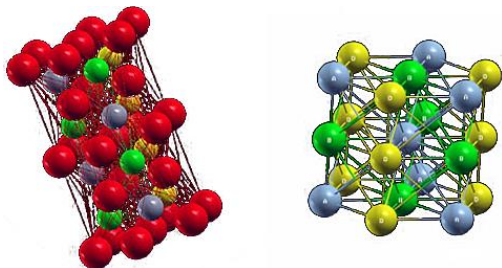

Fig. 2. Structure of ε-cementite [2]

The sublattice *a* is enriched in carbon, unlike sublattices *b* and *d*, and at low temperatures, the carbon atoms occupy only α -type pores. Within each close-packed plane, the pores form a trigonal lattice in which a pore of each type is positioned at the center of two equilateral triangles formed by the second and the third type pores, respectively, and these triangles and turned by 60° with respect to each other. Employing the ε-cementite model instead of the real, rhombic cementite is motivated not only by the simplicity considerations, but mainly by the following facts: (A) The rhombic Fe_3C can be obtained from the ε- Fe_3C via quite small displacements of several atoms Fe and C, (B) There are many indications that the austenite-cementite transformation is realized via the intermediate state ε-Fe_3C [2].

A transient phase Fe_2C with orthorhombic (η) or hexagonal (ε) structure has been reported. This phase was also called εFe_3C due to the uncertainty in the composition. Established that the structure of Fe_2C is an orthorhombic distortion of hexagonal ε. Though the hexagonal ε is in fact distorted to an orthorhombic form η, the lattice parameters are reported in Table 1. Approximately, $a(ort) = \sqrt{3}a(hex)$, $b(ort) = c(hex)$, and $c(ort) = a(hex)$ [3].

The members of the hcp family, like θ-Fe_3C (the cementite phase) and η-Fe_2C (the Hägg phase) are essential in the processes of manufacturing. The calculations confirm that the stability order for the most important hcp phases is (from high value of stability to lower): η-Fe_2C > o-Fe_7C_3 > θ-Fe_3C. Worth noticing is the fact that both η-Fe_2C and ε-Fe_2C have similar Fe sublattices. The major difference is the ordering of C atoms. In η-Fe_2C, along the *c* axis the carbon atoms are forming the C-C bonds with the length of about 2.8 A°, while in ε-Fe_2C, the C atoms are forming the zigzagged chains with higher values of C-C bond lengths [4].

The distortion of the Fe sublattice in h-Fe_3C from the hcp arrangement was discussed by some scientists, while other researchers discussed the hcp-family crystal structure in the terms of lattice twinning [5].

The relationship in the structures exists between ε-Fe_2C and the other iron carbides, χ-Fe_5C_2, θ-Fe_3C, and the Fe_7C_3 phases. In χ-Fe_5C_2 and θ-Fe_3C, the Fe atoms are in distorted sheets of hexagonal arrangements. Mentioned Fe hcp sheets are arranged in a zigzagged manners. This implies that strong relaxation of the Fe sublattices is required to transform from ε-Fe_2C to χ-Fe_5C_2 and θ-Fe_3C. Other one of important iron carbides with hcp Fe sublattices has composition Fe_7C_3. There are two phases: hexagonal (h-) and orthorhombic (o-). Theoretical calculations indicate that both phases stability values are close to the values of θ-Fe_3C cementite, and by implication to the o-Fe_7C_3, which is preferred by energy to the hexagonal variant h-Fe_7C_3. Both phases are related by structure and show similar Fe sheets. These sheets in o-Fe_7C_3 are also stacked in a zigzagged manner, which are similar to those in χ-Fe_5C_2 and θ-Fe_3C [5].

Table 1.
Lattice parameters of iron carbide [3]

Phase	Composition, at. %C	Lattice parameters, nm		
		a	b	c
Fe$_3$C(θ)	25	0,4526	0,5089	0,6744
		0,4527	0,5079	0,6750
At 21°C		0,45235	0,50890	0,67433
At 25°C		0,45246	0,50876	0,67401
At 18°C		0,45230	0,50890	0,67428
		0,45244	0,50885	0,67431
		0,4514	0,5084	0,6746
		0,451	0,5079	0,6730
		0,4526	0,5087	0,6744
		0,4525	0,5087	0,6741
		0,45255	0,5089	0,6744
		0,4516	0,5077	0,6727
		0,4523	0,5090	0,6748
Fe$_2$C(η)	33,3	0,4704	0,4318	0,2830
		0,470	0,429	0,285
Fe$_2$C(ε)	33,3	0,274	-	0,434
		0,2754	-	0,4349
		0,2756	-	0,4362
		0,2752	-	0,4354
		0,2794	-	0,4360
		0,2750	-	0,4353

2. Experimental procedure

The Fe-C sample was prepared from Armco and pressed graphite of spectral purity 99.99 %C in a corundum crucible under the protection of argon gas in Balzers-type heater. After dross removal and homogenization, the molten alloy was poured into permanent mold and cast into rod 12 mm in diameter. The specimen was then machined to approximately 5 mm in diameter using a wire cutting process because of the high brittleness of the metals at this composition. The chemical composition of this alloy is presented in Table 2.

The sample was positioned in a alunde tube with an inner diameter of 6 mm at the center of the vacuum Bridgman-type

furnace. Under an argon atmosphere, the sample was heated to a temperature of 1450°C. After stabilizing the thermal conditions, the sample was lowered at a given rate from the heating part to the cooling part of the furnace, with liquid metal used as the coolant.

Table 2.
Chemical composition of Fe-C alloy

Chemical composition wt. %					
C	Si	Mn	P	S	Cr
4,25	0,057	0,64	0,0079	0,021	0,033
Ni	Mo	Al	Cu	Co	Ti
0,0093	<0,0020	0,011	0,032	0,0024	<0,0010
Nb	V	W	Pb	Mg	B
<0,0040	0,0022	<0,010	<0,0030	<0,0010	0,0009
Sn	Zn	As	Bi	Ca	Ce
0,0061	<0,0020	0,0069	<0,0020	0,0005	<0,0030
Zr	La	Fe			
0,0043	0,0013	94,9			

The specimen was grown by pulling it downwards at a constant pulling rate v=83 μm/s and at a constant temperature gradient G=33,5 K/mm by means of motor. This is described in more detail in [6].

The directional solidification was performed in the Department of Casting at the AGH University of Science and Technology in Cracow. The EBSD (Electron Backscattered Diffraction) measurements were performed in Institute of Metallurgy and Materials Engineering - Polish Academy of Sciences in Cracow.

2.1. Microstructure research

After being mechanically ground, polished and etched with nital the microstructure of the sample was examined using a light optical microscope. The microstructure of sample was photographed on the longitudinal section.

Figure 3 show the polished and etched sample with marked growth direction. The eutectic microstructure on the Figure 4 is represented. The texture of the cementite matrix was observed.
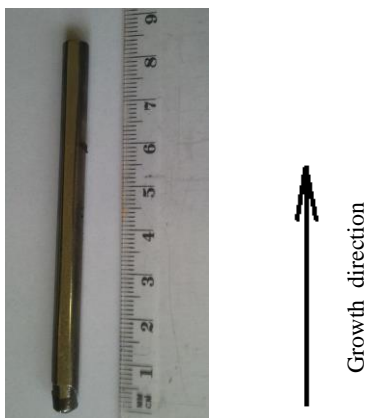
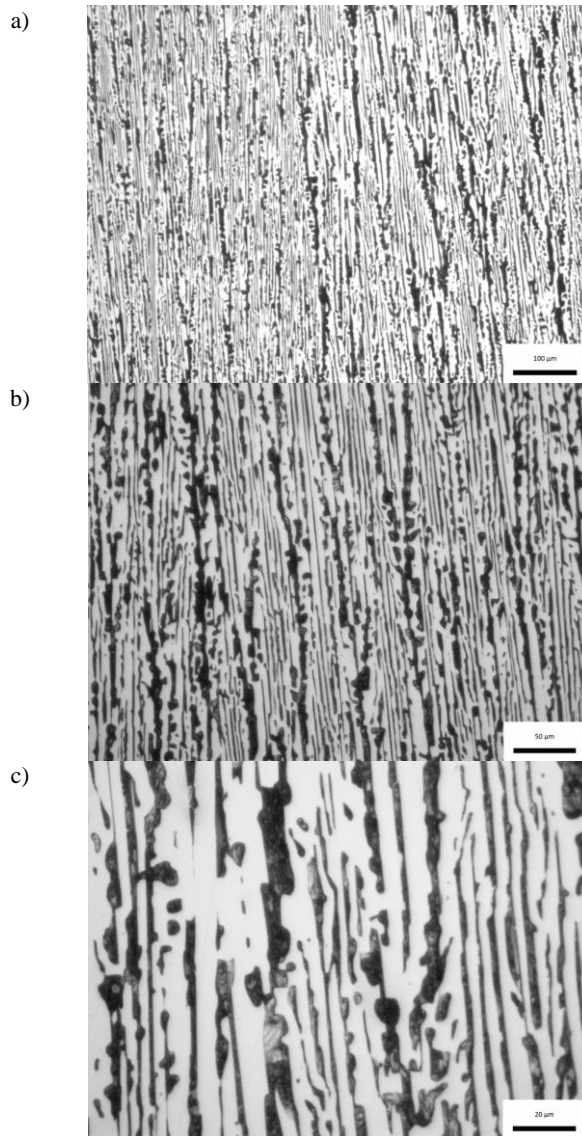Fig. 3. The image of the research sample

a)
b)
c)

Fig. 4. Microstructure of carbide eutectic on the longitudinal section: a) – 100x, b) – 200x, c) – 500x

2.2. X-ray diffraction

The directional solidification sample has been X-ray investigations. The X-ray diffraction studies of the sample of eutectic alloy were performed by means of Co Kα radiation.

The inspected surface, was longitudinal to the direction of growth during solidification. The measurement was made parallel and perpendicular to the axis of the goniometer

Radiation lamps with cobalt anode and an iron filter were used. Diffractograms were recorded in the 2θ angle range of 40÷80 with 0,02 steps. The radiation length was 0,179021 nm.

2.3. EBSD measurement

An automatic EBSD system is based on a SEM in combination with an EBSD detector. The detector consists of a phosphor screen and a charge coupled device (CCD) camera which is connected to a computer for image processing.

The electron backscatter diffraction technique is based on automatic diffraction patterns analysis. Which are composed of Kikuchi bands and are generated by interaction of a flat crystal surface with a vertical incident electron beam. The screen made of phosphor, located close to the thin section in order to collect the backscattered electrons as well as to emit a photonic image of the EBSD pattern.

By comparison of the observed Kikuchi bands pattern with those simulated for a pre-defined crystallographic structure the crystal orientation was determined.

3. Experimental results

A diffractograms from an X-ray diffraction are shows on the Figure 5÷8. Figure 6 show diffractometer trace performed in Institute of Metallurgy and Materials Engineering PAS in Cracow. Figure 6 show X-ray diffraction patterns, when the measurement was made parallel to the axis of the goniometer, Figure 7 parallel to the axis only for 50÷55 2θ angle, and Figure 8 - perpendicular to the axis.

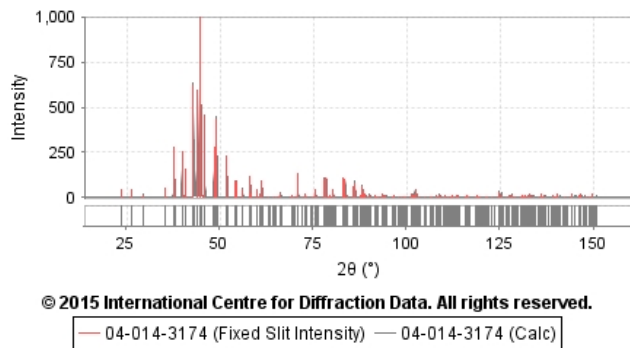— 04-014-3174 (Fixed Slit Intensity) — 04-014-3174 (Calc)

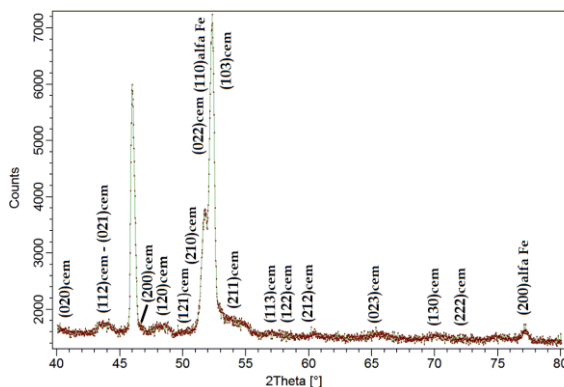Fig. 5. Diffractometer trace, PAS – Cracow

Fig. 6. Diffractometer trace parallel to the axis of the sample
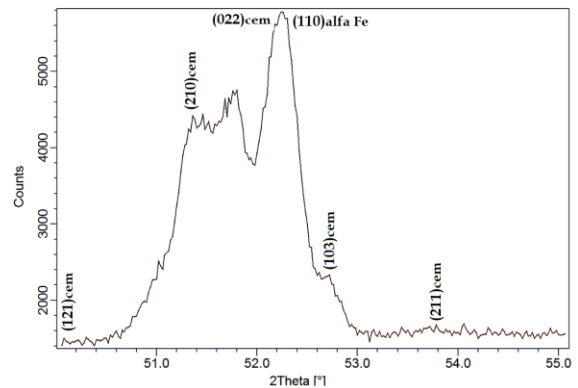

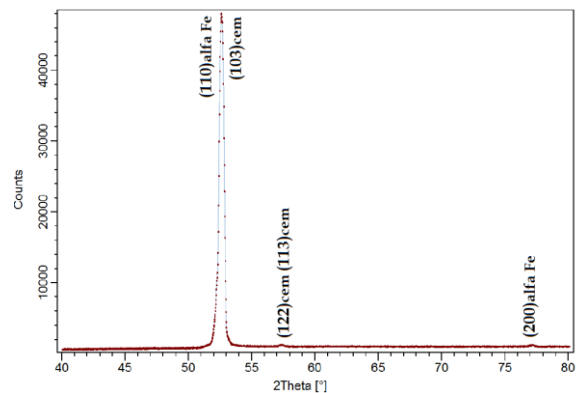Fig. 7. Diffractometer trace parallel to the axis of the sample for 50÷55 2θ

Fig. 8. Diffractometer trace perpendicular to the axis of the sample

Figure 9 show microstructure of carbide eutectic, phase map, and phase analysis of this structure.

A diffraction pattern records the X-ray intensity as a function of 2θ angle.

5. Analysis of results

Results of X-ray diffraction research are presented in Table 3. Presentation of the phase fraction is shown in Table 4.

The calculated values lattice parameter of cementite were listed in Table 5. Values in italics are calculated on the basis of indicators *(hkl)*, other values were calculated based on the formulas of [7].

Table 3 show, that the in analyzed areas parallel and perpendicular to the axis of sample, different results of X-ray diffraction were obtained. This applies to the occurrence of the peaks and their intensity values. Many reflections of cementite were observed on the diffraction trace parallel to the axis of the sample (Fig. 6 and Fig. 7). On the contrary, the diffractometer trace perpendicular to the axis (Fig. 8) only one strong and two weak peak of cementite occurred.

The EBSD measurements (Fig. 9 and Tab. 4) show the existence of iron carbide with orthorhombic (θ) and hexagonal (ε) structure.
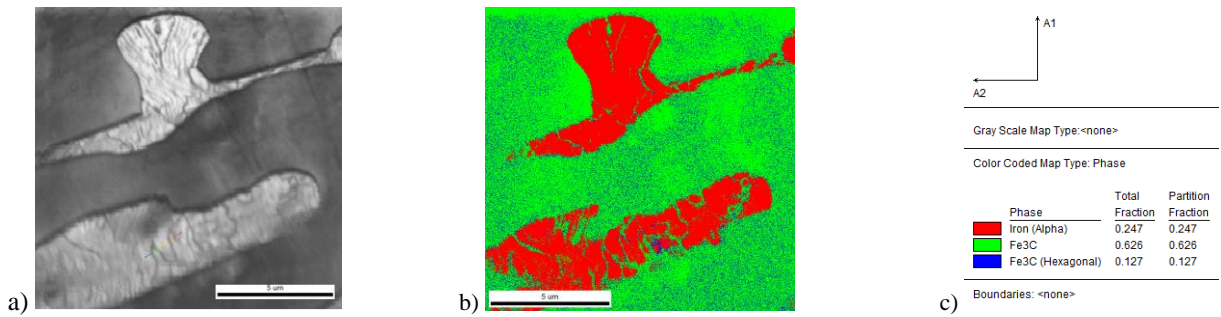
Fig. 9. Microstructure of carbide eutectic: a) SEM image, b) phase map (EBSD), c) analysis of phase (EBSD), v=300 mm/h

Table 3.
X-ray diffraction results

	Research of parallel to the axis (Fig. 7)			Catalog of reflections list [8]					
				θ-Fe$_3$C			αFe		
Peak	2θ	d_{hkl}	I/I_{max}	d_{hkl}	hkl	I/I_{max}	d_{hkl}	hkl	I/I_{max}
1	40,90	2,5609	22	2,54185	020	1,7			
2	43,84	2,3961	24						
3	44,00	2,3878	24	2,38655	112	27			
4	44,16	2,3796	24	2,37867	021	25,9			
5	46,74	2,2550	23	2,25825	200	24			
6	45,98	2,2902	83						
7	48,10	2,1949	23	2,21514	120	19,2			
8	48,46	2,1795	24						
9	50,34	2,1032	22	2,10463	121	53,4			
10	51,36	2,0641	61	2,06379	210	50,7			
11	51,80	2,0478	52						
12	52,26	2,0310	92	2,03014	022	48,6			
13	52,34	2,0281	100				2,0268	110	100
14	52,76	2,0131	100	2,01333	103	100			
15	53,90	1,9737	24	1,97354	211	48,2			
16	57,12	1,8710	22	1,87188	113	30			
17	57,66	1,8555	21	1,85168	122	53,4			
18	60,36	1,7793	22	1,76052	212	18,4			
19	65,42	1,6550	22	1,68442	023	13			
20	70,10	1,5575	22	1,58657	130	15,5			
21	72,44	1,5138	20	1,50975	222	9			
22	77,20	1,4337	22				1,4332	200	19
	Research of parallel to the axis for 50÷55 2θ (Fig. 8)			Catalog of reflectoins list [8]					
				θ-Fe$_3$C			αFe		
Peak	2θ	d_{hkl}	I/I_{max}	d_{hkl}	hkl	I/I_{max}	d_{hkl}	hkl	I/I_{max}
1	50,30	2,1047	26	2,10463	121	53,4			
2	51,02	2,0770	44						
3	51,36	2,0641	76	2,06379	210	50,7			
4	51,46	2,0604	77						
5	51,68	2,0255	80						
6	51,80	2,0478	82						
7	52,24	2,0318	100	2,03014	022	48,6	2,0268	110	100
8	52,72	2,0146	40	2,01333	103	100			
9	53,80	1,9770	28	1,97354	211	48,2			
10	54,06	1,9683	29						
	Research of perpendicular to the axis (Fig. 9)			Catalog of reflectoins list [8]					
				θ-Fe$_3$C			αFe		
Peak	2θ	d_{hkl}	I/I_{max}	d_{hkl}	hkl	I/I_{max}	d_{hkl}	hkl	I/I_{max}
1	52,62	2,0181	100	2,01333	103	100	2,0268	110	100
2	57,38	1,8632	3	1,87188	113	53			
				1,85168	122	30			
3	77,16	1,4344	3				1,4332	200	19

6. Conclusions

The analyse of results of X-ray diffraction shows, that not all of the peaks have been identified (Fig. 6: peaks 2, 6, 8, 11 and Fig.7: peaks 2, 4, 5, 6, 10). This identification is impossible to obtain also with the EBSD research methods. Unidentified peaks can be derived from the close arrangement fraction of nanocrystallites. They may come from other iron carbides (ε-Fe_2C, χ-Fe_5C_2, Fe_7C_3). These unrecognized peaks may also be a result of the residual impurity of alloy.

Table 4.
The measurements results of phase fraction (EBSD)

Phase	Measurement				
	1	2	3	4	average
Fe(α)	0,247	0,263	0,335	0,371	0,30400
Fe_3C orthorhombic	0,626	0,620	0,532	0,509	0,57175
Fe_3C hexagonal	0,127	0,118	0,133	0,121	0,12475

Table 5.
Values of *a, b, c* lattice parameter of cementite

References	*a*, nm	*b*, nm	*c*, nm
[8]	0,45165	0,50837	0,67475
[9]	0,5076	0,4514	0,6757
[10]	0,48190	0,64774	0,42805
	0,50080	0,67254	0,44650
[11]	0,5092	0,6741	0,4527
[12]	0,45246	0,50884	0,67423
[13]	0,45310		
	0,45369	*0,51596*	0,67556
[13]	*0,45356*		*0,677*
	0,4534	0,50962	0,68090
[13]	*0,45404*		*0,67652*
	0,45434	0,50954	0,68012
[PAS]	0,451933	0,510096	0,677706
	0,75650	0,49718	0,68340

The arrangement of the sample relative to the goniometer axis was parallel and perpendicular. Diffraction pattern taken perpendicularly to the axis of the sample (Fig. 8) do not show many peaks. This may suggest the existence of carbide eutectic texture formed during the directional solidification. Structure of the texture can be seen on Figure 4.

EBSD studies show no deformation of iron carbide lattice plane. Instead, the existence of iron carbide with hexagonal and orthorhombic structure, was revealed.

Based on the reports from the introduction, the presence of the hexagonal iron carbide can be caused by lack of possibility to convert it into orthorhombic iron carbide, due to the high pulling rate in directional solidification.

References

[1] Gholizadeh, H. (2013). *The influence of alloying and temperature on the stacking-fault energy of iron-based alloys*. Dissertation, Leoben.

[2] Khromov, K.Yu. & Vaks, V.G. (2008). On the theory of phase equilibria austenite cementite in steel and on interactions of carbon atoms in FCC and HCP iron. *Journal of Experimental and theory Physics.* 106(2), 265-279.

[3] Okamoto, H. (1992). The C-Fe (Carbon-Iron) System, *Journal of Phase Equilibria.* 13(5).

[4] Fang, C.M., van Huis, M.A., Thijsse, B.J. & Zandbergen, H.W. (2012). Stability and crystal structures of iron carbides, *Physical Review.* B 85, 054116.

[5] Fang, C.M., van Huis, M.A. & Zandbergen, H.W. (2010). Structure and stability of Fe_2C phases from density-functional theory calculations. *Scripta Materialia.* 63, 418-421.

[6] Trepczyńska-Łent, M. (2013). Possibilities of the materials properties improvement for the cementite eutectic by means of unidirectional solidification. *Archives of Metallurgy and Materials.* 58(3), 987- 991.

[7] Senczyk D. (1974). *Laboratory of X-ray crystallography.* Poznań: Wydawnictwo Uczelniane Politechniki Poznańskiej 205 (in Polish).

[8] www.msm.cam.ac.uk/phase-trans/2003/Lattices2/cementite. data.txt

[9] Battezzati, L., Baricco, M., Curiotto, S. (2005). Non-stoichiometric cementite by rapid solidification of cast iron. *Acta Materialia.* 53, 1849-1856.

[10] Lv, Z.Q., Zhang, F.C., Sun, S.H. & other (2008). First-principles study on the mechanical, electronic and magnetic properties of Fe_3C. *Computational Materials Science.* 44, 690-694.

[11] Herbstein, F.H., Smuts, J. (1964). Comparison of X-ray and neutron-diffraction refinements of the structure of cementite Fe_3C. *Acta Crystallographica.* 17, 1331-1332.

[12] Stuart, H., Ridley, N. (1966). Thermal expansion of cementite and other phases. *Journal of the Iron and Steel Institute.* 711-717.

[13] Trepczyńska-Łent, M. & Szykowny, T. (2015). X-ray diffraction study of directional solidification ledeburite. *Archives of Foundry Engineering.* 15(3), 71-76.